Clinical Chemistry 51:10
1914–1922 (2005)

Oak Ridge Conference

Plasmonic Technology: Novel Approach to Ultrasensitive Immunoassays

Joseph R. Lakowicz,* Joanna Malicka, Evgenia Matveeva, Ignacy Gryczynski, and Zygmunt Gryczynski

At the Center for Fluorescence Spectroscopy, we have taken advantage of the favorable properties of surface plasmon-coupled emission (SPCE) to improve fluorescence-based immunoassays. SPCE occurs when excited fluorophores near conducting metallic structures efficiently couple to surface plasmons. These surface plasmons, appearing as free electron oscillations in the metallic layer, produce electromagnetic radiation that preserves the spectral properties of fluorophores but is highly polarized and directional. SPCE immunoassays provide several advantages over other fluorescence-based methods. This review explains new approaches to fluorescence immunoassays, including our own use of SPCE for simultaneous detection of more than one fluorescent marker and performance of immunoassays in the presence of an optically dense medium, such as whole blood.

Biological markers in physiologic fluids are very useful tools in clinical diagnostics. Sensitive and reliable detection of specific biomarkers is crucial in disease identification, therapy, and patient screening. Reliable and quick detection of low concentrations of markers is particularly important in a disease such as acute myocardial infarction (AMI).[1] Myoglobin (Myo), although not completely cardiac specific, is one of the earliest markers to increase after AMI *(1–6)* and has been recommended for use in combination with other markers, such as creatine kinase-MB, troponin I, and troponin T, as an early diagnostic indicator for AMI *(1, 7–10)*. The immunoassay technique is widely used in this procedure *(11)*.

Immunoassay based on fluorescence detection is one approach to high-sensitivity detection of biomarkers *(12–16)*. Different fluorescence detection approaches include polarization *(17–21)*, resonance energy transfer *(22–24)*, and time-resolved gated assays based on long-lived lanthanide emission *(25–28)*. New approaches to fluorescence immunoassays are being developed, including multiphoton excitation *(29–31)*, with the emphasis on high-throughput immunoassays *(32–35)*.

The sensitivity of fluoroimmunoassays is typically limited by background fluorescence, which is present in most biological samples and in the optical elements of the instrumentation. In this report, we describe a new immunoassay format that provides increased sensitivity and background rejection by efficient light collection of emissions occurring near the bioaffinity surface. In this approach, a fluorescently labeled reporting molecule (antibody) is bound near a metallic surface, and the binding produces a highly directional and polarized emission. This effect is based on the resonant coupling of excited fluorophores with collective electron motions/oscillations at the interface between a thin metal film (typically silver or gold) and a dielectric bulk material. The so-called surface plasmons comprise an electromagnetic wave confined to the interface between the metal film and the transparent medium, and the electromagnetic wave of the surface plasmons is coupled to oscillations of free electrons in the metal.

A strong evanescent field induced by surface plasmons can excite a layer of fluorophores that extends up to ~200 nm above a thin metallic film into the liquid sample. We demonstrated recently that the reverse process is also possible; i.e., excited fluorophores near the metallic layer may induce surface plasmons in the metallic film, which

Center for Fluorescence Spectroscopy, Department of Biochemistry and Molecular Biology, University of Maryland School of Medicine, Baltimore, MD.

*Address correspondence to this author at: Center for Fluorescence Spectroscopy, Department of Biochemistry and Molecular Biology, University of Maryland School of Medicine, 725 West Lombard St., Baltimore, MD 21201. Fax 410-706-8408; e-mail lakowicz@cfs.umbi.umd.edu.

Received April 25, 2005; accepted May 27, 2005.

Previously published online at DOI: 10.1373/clinchem.2005.053199

[1] Nonstandard abbreviations: AMI, acute myocardial infarction; Myo, myoglobin; SPCE, surface plasmon-coupled emission; RK, reverse Kretschmann; KR, Kretschmann; and LOD, limit of detection.

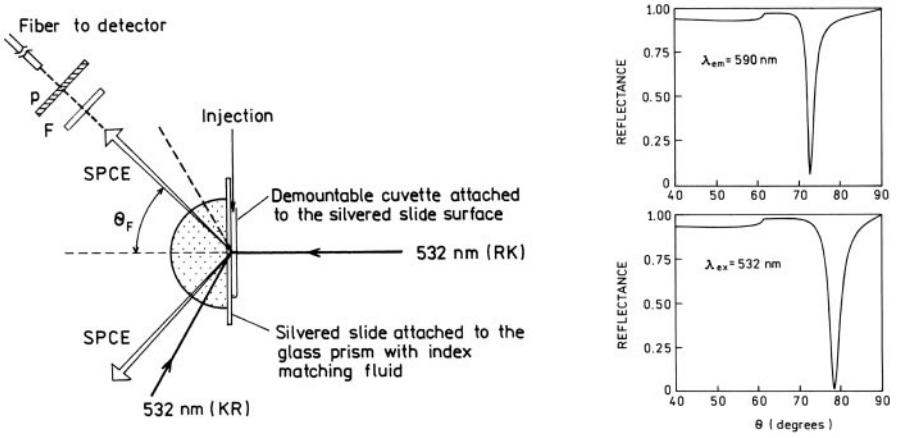

Fig. 1. Experimental geometry for measurements of SPCE emission with RK and KR configurations (*left*), and calculated reflectivity curves for a 50-nm silver film on BK7 glass ($n_p = 1.52$; *right*).

(*Right*), the sample (protein layers) was assumed to be 18 nm thick ($n_s = 1.50$). The buffer thickness was taken as infinite with $n_w = 1.33$. For the silver phase, we used dielectric constant $\epsilon_m^{532} = -11.5 + 0.3i$, and $\epsilon_m^{590} = -15.0 + 0.4i$. Adapted from Matveeva et al. *(54)*.

radiate into the glass substrate *(36, 37)*. This radiation occurs at a sharply defined angle and is almost completely polarized. This phenomenon, which we call surface plasmon-coupled emission (SPCE), appears to be closely related to surface plasmon resonance *(36, 38–40)*. The interaction between the excited fluorophores and the metal causes coupling of the energy quanta to a 2-dimensional electromagnetic wave at the interface between metal and glass. In turn, this electromagnetic wave is coupled to oscillations of electrons in the metal, which can then radiate an electromagnetic field into the glass. The interaction of excited dipoles with metal is a near-field resonance effect occurring without the emission of photons, similar to the Förster resonance energy transfer mechanism; however, detailed studies of the mechanism are still needed.

Surface plasmon resonance occurs when light impinges on a thin metal film through a medium with a higher refractive index. Resonance occurs only at a specific angle of incidence (θ_{SP}) that satisfies exactly the wave vector–matching conditions. At this angle of incidence, the surface plasmons are excited, producing a sharp reflectivity decrease (Fig. 1, right). We found that plasmons created by nearby excited fluorophores may cause radiation into the glass substrate at the surface plasmon angle (θ_F) that satisfies the wave vector–matching conditions for the emission wavelengths.

There are 2 possible experimental configurations for SPCE excitation. First, the sample can be illuminated from the sample side, which is the so-called reverse Kretschmann (RK) configuration. In this case, the excitation cannot generate surface plasmons in the metal surface. The sample can also be illuminated through a prism at the plasmon resonance angle (θ_{SP}), which is called the Kretschmann (KR) configuration (Fig. 1, left). If the incident angle $\theta_I = \theta_{SP}$, then the excited surface plasmons induce an evanescent field above the metal film surface. This evanescent field, which is strongly enhanced (up to 80-fold compared with the incident field) by the resonance interaction *(41)*, extends up to ~200 nm into the liquid sample. Hence, the KR illumination leads to a strong selective excitation in close proximity to the metal surface. The enhanced excitation field is confined to the evanescent layer, effectively reducing the background from the sample volume matrix. The exceptional sensitivity of SPCE-based assays has been observed in our and other laboratories *(42–48)*.

Model SPCE Immunoassay

We used SPCE to develop a model affinity assay with labeled goat anti-rabbit IgG antibodies against rabbit IgG bound to a 50-nm thick silver film *(48)*. Rhodamine Red-X–labeled IgG was placed near the silver surface by its binding to the surface-bound antigen (Fig. 2, left). The sample was illuminated in the RK configuration, which does not create surface plasmons in response to the incident light. We measured the emission intensity for all accessible angles from the normal axis. The intensity observed through the prism was sharply directed near ±75 degrees (Fig. 2, right). This value is consistent with that calculated from minimum reflectance for p-polarized plasmon mode for a 595 nm emission wavelength *(49)*.

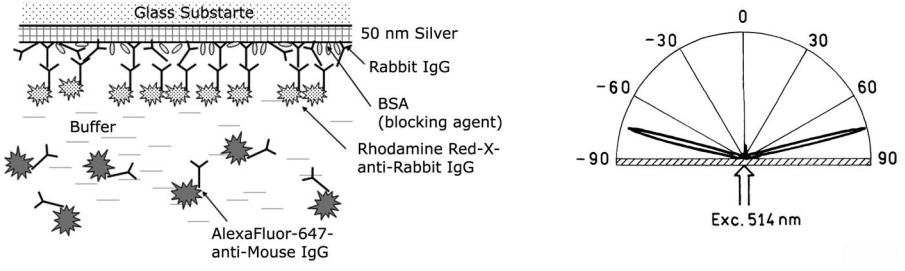

Fig. 2. Binding of labeled antibodies to the beads.

(*Left*), anti-rabbit antibodies (labeled with Rhodamine Red-X) bind to rabbit IgG immobilized on the silver surface; the nonbinding anti-mouse antibodies labeled with AlexaFluor-647 remain in solution (drawing is not to scale). *BSA*, bovine serum albumin. (*Right*), angular distribution of the 595 nm fluorescence emission of Rhodamine Red-X–labeled anti-rabbit antibodies bound to the rabbit IgG immobilized on the 50-nm silver mirror surface. Adapted from Matveeva et al. *(48)*.

The emission spectrum of the SPCE was characteristic of the rhodamine probe (Fig. 3, bottom), and the spectrum was not corrupted by scattered light at the excitation wavelength.

We tested the use of SPCE to monitor the binding kinetics of rhodamine-labeled antibodies to the surface-bound antigen. The emission intensities after addition of labeled antibody are shown in the top panel of Fig. 3. The emission climbs rapidly and reaches a limiting value. It is important to recognize that this 10-fold change in intensity is not produced by a change in the rhodamine quantum yield on binding but by transport of the rhodamine molecules to be near the metal film. We measured the effect of binding of rhodamine-labeled goat antibody to the antigen while both were free in solution and found that the intensity decrease attributable to binding was ~25%. This result further demonstrates that the intensity change is a product of probe localization in the evanescent field near the silver. The use of SPCE thus is a generic method for detection of surface localization by a change in intensity but does not require a change in the fluorophore quantum yield on binding.

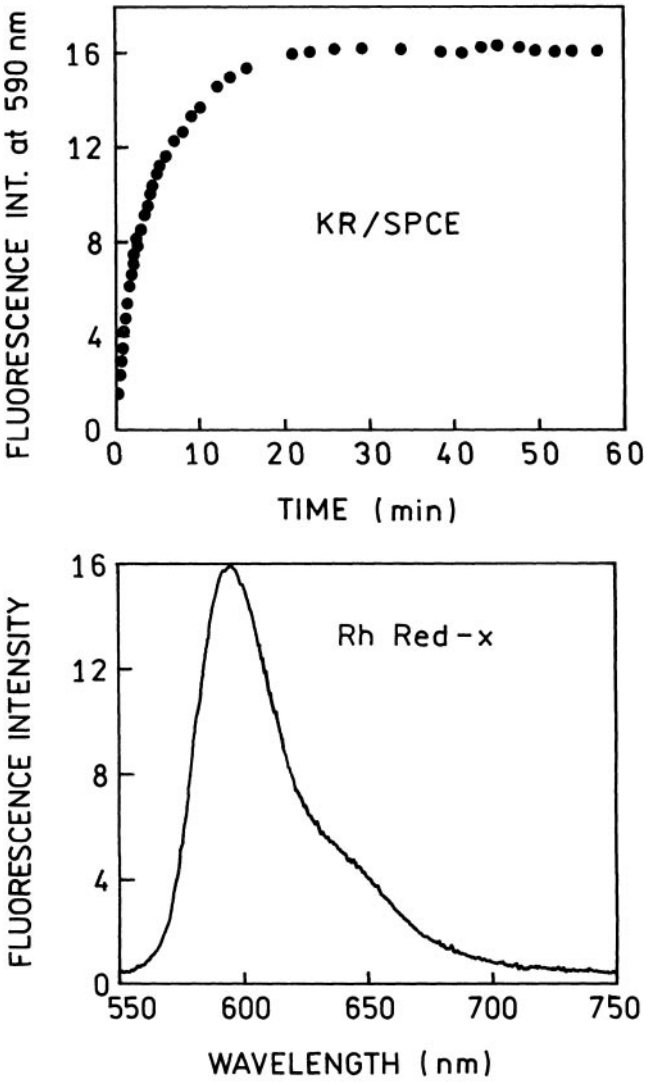

Fig. 3. Binding kinetics of the Rhodamine Red-X–labeled anti-rabbit antibodies bound to rabbit IgG immobilized on a 50-nm silver mirror surface observed with KR/SPCE configuration (*top*), and emission spectrum measured after 60 min (*bottom*).

INT, intensity. Adapted from Matveeva et al. *(48)*.

Advantages of SPCE-Based Immunoassays

BACKGROUND SUPPRESSION

We tested several optical configurations to determine the relative intensities and extent of background rejection possible with SPCE *(48)*. These 3 configurations are shown in the right-hand panels in Fig. 4. The sample consisted of the surface saturated with Rhodamine Red-X–labeled antibody. AlexaFluor-647–labeled antibody solution (which had no affinity to the surface) was added to mimic autofluorescence from the sample. The 0.03 μmol/L concentration of this antibody (0.13 μmol/L Alexa dye) produced dominant free-space fluorescence signal from the sample at 670 nm. The sample was first

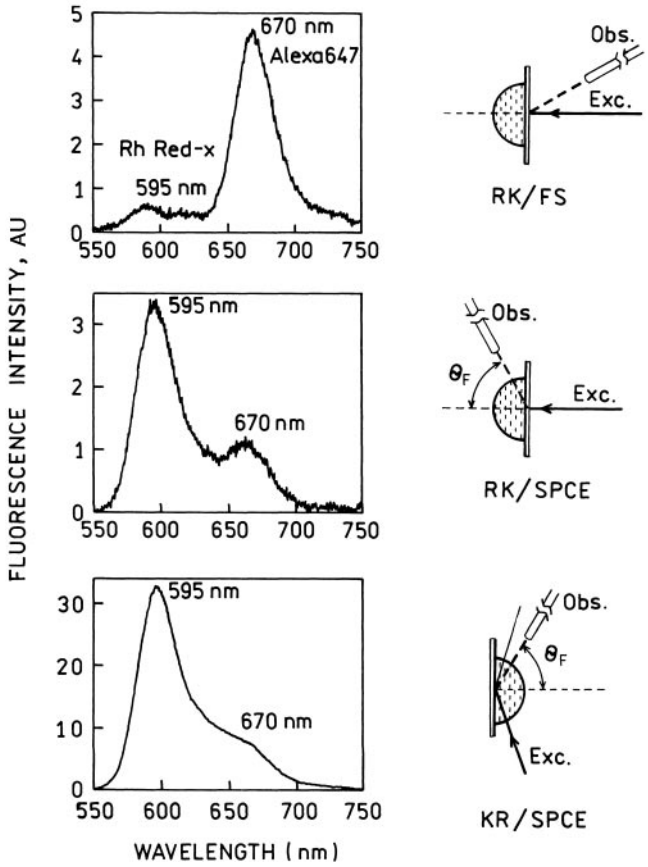

Fig. 4. Emission spectra of the Rhodamine Red-X–labeled anti-rabbit antibodies bound to rabbit IgG immobilized on a 50-nm silver mirror surface in the presence of a fluorescent background (anti-mouse antibodies labeled with AlexaFluor-647) measured with different optical configurations.

AU, arbitrary units; *Exc*, excitation; *Obs*, observed. Adapted from Matveeva et al. *(48)*.

excited using the RK configuration, and the free-space emission was observed from the same water side of the sample (Fig. 4, top panel). Compared with subsequent measurements (below), the intensity of the desired rhodamine antibody was weak. The free-space emission was dominated by the emission from Alexa at 670 nm, with only weak rhodamine emission at 595 nm. We then measured the emission spectrum of the SPCE signal (Fig. 4, middle panel), while still using RK illumination. The emission spectrum was dramatically changed from a 10 to 1 excess of the unwanted background to a 5 to 1 excess of the desired signal. The use of SPCE therefore allowed selective detection of the rhodamine-labeled antibody near the silver film.

We next changed the mode of excitation to the KR configuration (Fig. 4, bottom panel). In this case, the sample was illuminated at $\theta_{SP,}$ creating an evanescent field in the sample. This increased overall intensity 10-fold and further suppressed the unwanted emission from AlexaFluor-647. The increased intensity and decreased background are the products of localized excitation by the resonance-enhanced field near the metal. In this case, the emission was produced almost entirely by the rhodamine, with just a minor contribution from the Alexa-labeled protein. In our opinion, SPCE-based immunoassays provide unprecedented background rejection with a simple optical configuration and without electronic gating.

MULTICOLOR IMMUNOASSAYS

The SPCE phenomenon offers intrinsic wavelength resolution, which can be used in multicolor immunoassays. The experimental configuration for 2-wavelength SPCE *(50)* is shown in the top panel of Fig. 5. The silver surface, coated with a mixture of Rhodamine Red-X–labeled and AlexaFluor-647–labeled antibodies, was illuminated at the surface plasmon angle through the glass prism (KR configuration) by 532 nm light, which excites both dyes. The free-space emission was normal to the sample surface, on the side distal from the prism, with a filter and a fiber optic bundle. SPCE was observed on the prism side of the sample at 2 different angles through appropriate long-pass filters for each labeled antibody (595 nm for the Rhodamine Red-X–labeled antibody and 665 nm for the AlexaFluor-647–labeled antibody).

To preadjust the optical setup, we calculated the reflectivity curves with available software *(51, 52)*. The reflectivity minima were at 72.5 degrees for 532 nm, and at 69 and 67 degrees for 595 and 665 nm, respectively (Fig. 5, bottom). We thus expected to obtain excitation of surface plasmons with a 532 nm incident angle of ~72.5 degrees and to observe the emissions for the Rhodamine Red-X– and AlexaFluor-647–labeled antibodies at 69 and 67 degrees, respectively.

We examined the angle-dependent emission intensity for an antigen (rabbit IgG)-covered surface, which was saturated with a mixture of Rhodamine Red-X– and AlexaFluor-647–labeled antibodies (Fig. 6, left). The emission from both labeled antibodies was strongly directional at different angles on the prism, as expected. The emission from rhodamine peaked at 71 degrees and that from Alexa dye at 68 degrees.

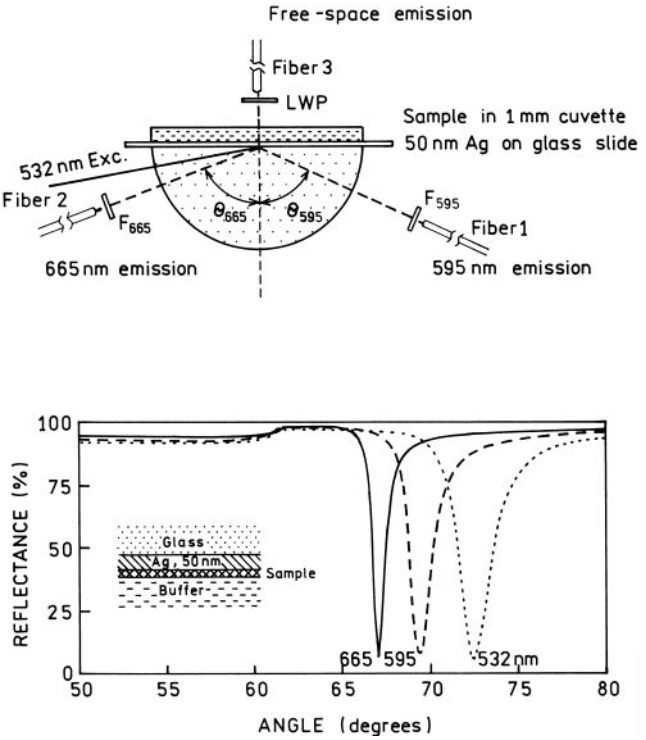

Fig. 5. Experimental configuration for the 2-color SPCE assay with surface plasmon (Kretschmann) excitation (*top*), and calculated reflectivity of a 50-nm silver film on BK7 glass ($n_p = 1.52$; *bottom*).

(*Top*), fibers 1 and 2 collect SPCE at 595 nm and 665 nm, respectively. Fiber 3 observes the free-space emission. *LWP*, long wavelength pass filter. (*Bottom*), the sample (protein layers) was assumed to be 15 nm thick ($n_s = 1.50$). The buffer thickness was taken as infinite with $n_w = 1.33$. For the silver phase, we used dielectric constant $\epsilon_m^{532} = -11.5 + 0.3i$; $\epsilon_m^{595} = -15.0 + 0.4i$; and $\epsilon_m^{665} = -21.0 + 0.6i$. Adapted from Matveeva et al. *(50)*.

We used SPCE at 2 observed angles to simultaneously measure the binding kinetics of both labeled antibodies (Fig. 6, right). The binding kinetics were similar, although the final intensities were different (Fig. 6, ▲ and △). The binding was also measured by use of KR excitation and the free-space emission (Fig. 6, ● and ○). The intensities were >10-fold higher for SPCE than for the free-space emission. The SPCE-based immunoassay therefore provides better resolution for a multicolor/multianalyte system than a system for which free-space emission is observed. The SPCE immunoassays offer the opportunity to simultaneously observe of multiple fluorescent markers.

SPCE IMMUNOASSAY IN OPTICALLY DENSE MEDIA

In medical testing, it is often desirable to perform homogeneous assays without separation steps, sometimes in whole blood. We reasoned that an SPCE signal should be detectable in optically dense media because this signal arises from the sample within 200 nm of the surface.

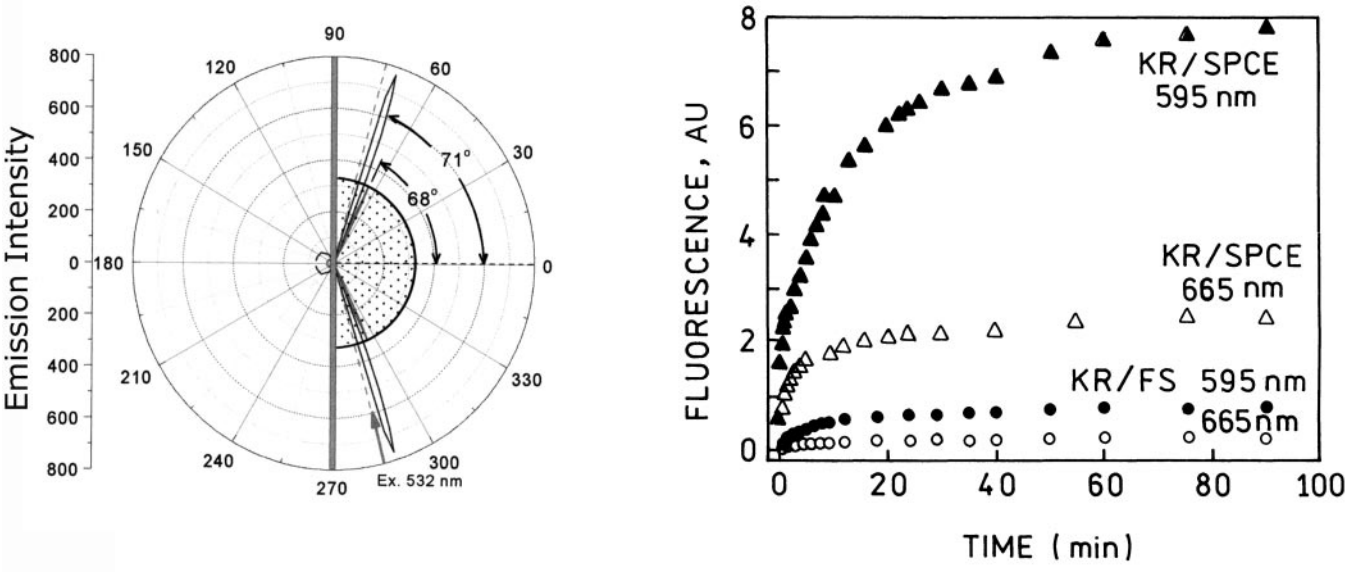

Fig. 6. Angle-dependent emission from a surface containing Rhodamine Red-X– and AlexaFluor-647–labeled antibodies (*left*), and surface binding kinetics for SPCE emission (*right*).

(*Left*), emission was measured at 595 or 665 nm. The sample was excited at 532 nm and 75 degrees with the KR configuration. (*Right*), surface binding kinetics for the SPCE emission (▲ and △), observed as shown in the top panel of Fig. 5, at 71 degrees for 595 nm and −68 degrees for 665 nm. ● and ○, free-space emission. *AU*, arbitrary units. Adapted from Matveeva et al. *(50)*.

In the endpoint experiment, AlexaFluor-647–labeled anti-rabbit IgGs were first bound to rabbit IgGs immobilized near the silver surface (Fig. 7, left) *(53)*. The excess of nonbound antibodies was then washed away, and a sample matrix was added (serum, whole blood, or blocking solution for comparison), followed by measurements of the fluorescent signal and spectrum. We found that the emission was strongly directional and focused near an angle of 58 degrees. The spectrum of the SPCE (in KR configuration) was characteristic of the AlexaFluor-647 probe and not corrupted by scattered light at the excitation wavelength for all tested sample matrixes (Fig. 7, right). The whole blood sample used for this measurement had an absorbance of ~2.5 at 665 nm (emission maximum of the tested dye AlexaFluor-647) at the optical pathlength of 0.2 mm (as used for the SPCE experiment).

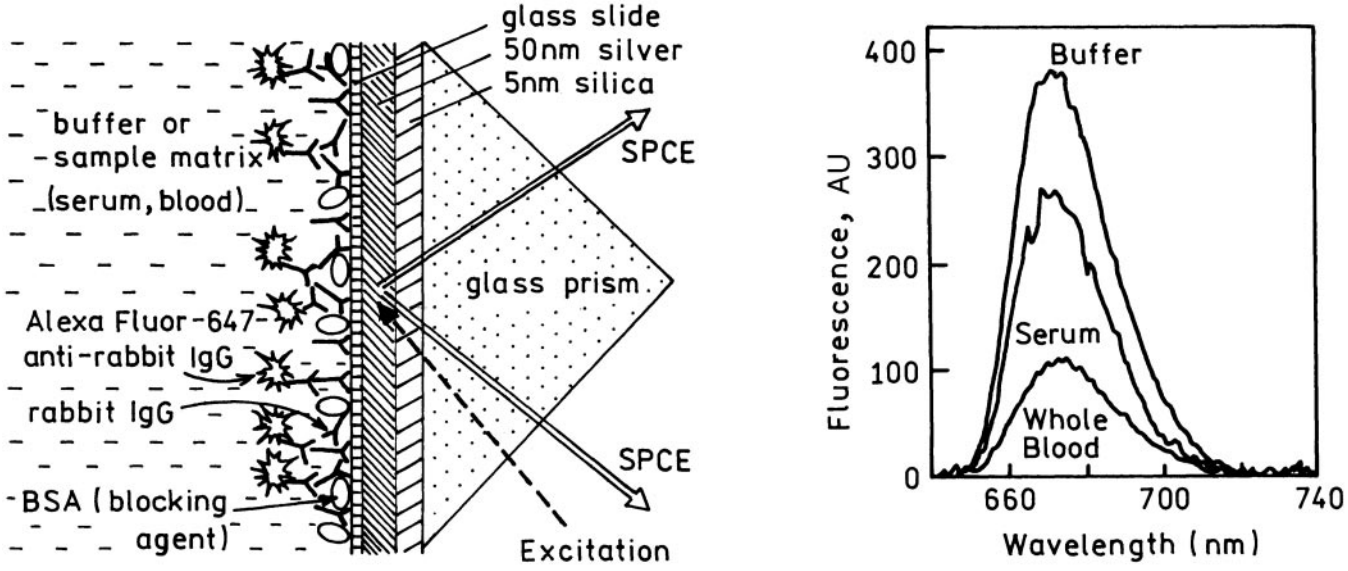

Fig. 7. Scheme of SPCE model immunoassay performed in optically dense medium (*left*), and surface plasmon-coupled emission spectra of the AlexaFluor-647–labeled anti-rabbit antibodies bound to the rabbit IgG immobilized on a 50-nm silver mirror surface in buffer, human serum, and human whole blood in KR/SPCE configuration (*right*).

BSA, bovine serum albumin; *AU*, arbitrary units. Adapted from Matveeva et al. *(53)*.

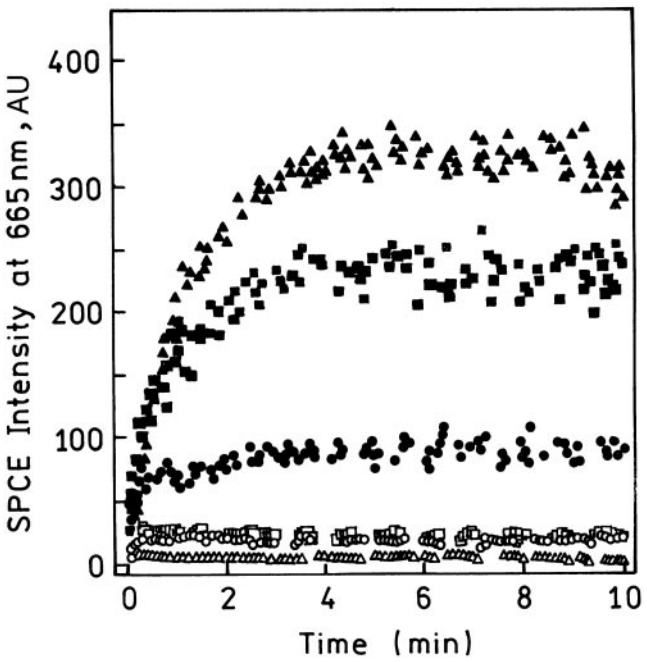

Fig. 8. Kinetics of the binding of the AlexaFluor-647–labeled anti-rabbit antibodies to the rabbit IgG immobilized on a 50-nm silver mirror surface.

Signal observed with the SPCE/KR configuration for buffer (▲), human serum (■), and human whole blood (●). Nonspecific kinetics (nonspecific binding of the AlexaFluor-647–labeled anti-rabbit antibodies to the immobilized goat IgG) are also shown: △, buffer control; □, serum control; ○, whole blood control. Adapted from Matveeva et al. *(53)*. *AU*, arbitrary units.

This absorbance in a 0.2-mm–thick blood sample would attenuate the fluorescence signal $\sim 10^{2.5}$-fold under free-space conditions. As shown in the right-hand panel of Fig. 7, with SPCE generation and detection, the signal was attenuated <2-fold in a human serum sample and ~3-fold in a whole blood sample compared with the transparent buffer medium (blocking solution). These results demonstrate the potential of SPCE in optically dense samples.

To characterize the effect of serum and whole blood on the SPCE signal, we estimated the limit of detection (LOD) as the concentration of labeled IgG (binding to the immobilized antigen) giving the same SPCE signal as the blank measurement (0 concentration of labeled antibodies) plus 3 SD, assuming linearity between 0 and 70 nmol/L (10 mg/L) of labeled IgG. In our model immunoassay, we estimated a 3- to 5-fold increase in LOD for serum and a 5- to 10-fold increase in LOD for whole blood.

In addition, we were able to monitor the binding process, which itself could be affected by the presence of serum or whole blood (Fig. 8). The increase of the signal evidently can be correlated with specific binding, as shown in Fig. 8. Nonspecific binding of the labeled anti-rabbit IgG to the wrong antigen (goat IgG) leads to an SPCE signal that does not change with time. We believe that the ability to perform assays in whole blood can speed up and simplify clinical assays.

SPCE Myo Immunoassay

To demonstrate usefulness of the SPCE-based immunoassay format for detection of a cardiac marker *(54)*, we performed the assay schematically depicted in Fig. 9 (left), in which Rhodamine Red-X–labeled antibody was bound to Myo immobilized near the silver surface. The emission spectrum of the SPCE was characteristic of the Rhodamine Red-X probe (Fig. 9, right). A remarkable characteristic of SPCE is almost complete polarization in the p direction, meaning that the electric vector is oriented parallel to the plane of incidence. The right-hand panel of

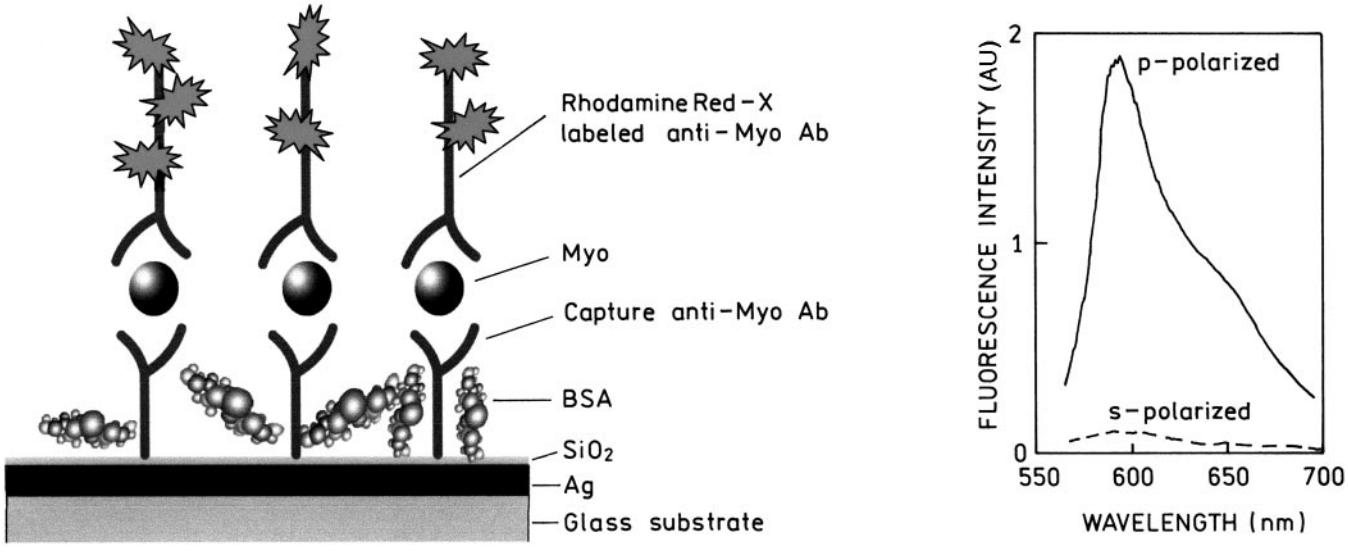

Fig. 9. Myo assay format.

(*Left*), scheme of the Myo immunoassay (sandwich format) on a thin silver mirror slide surface (drawing is not to scale). The thickness of the silver layer was 50 nm, and the SiO_2 protective layer was 5 nm thick. *BSA*, bovine serum albumin; *Ab*, antibody. (*Right*), polarized fluorescence spectra of the Rhodamine Red-X–labeled anti-Myo antibodies bound to the captured Myo observed at 72 degrees in RK/SPCE configuration. *AU*, arbitrary units. Adapted from Matveeva et al. *(53)*.

Fig. 9 shows the emission spectra collected through an emission polarizer (oriented p or s). This p polarization demonstrates that the emission is the product of surface plasmons that under these conditions cannot emit s-polarized light. An emission polarizer in the p orientation can be used to further suppress part of the free-space emission that can be transmitted through the metal film, some of which will display s polarization. We measured the sample emission with RK and KR configurations. The spectrum of Rhodamine Red-X–labeled antibody was the same in both cases.

For the KR configuration, the 532 nm excitation was at an angle of 74.5 degrees, which we found yielded the highest SPCE fluorescence. The emission was strongly directional at the angle 72 degrees. With these optical conditions, we measured the binding kinetics of the Rhodamine Red-X–labeled anti-Myo antibodies to the surface-bound Myo at various Myo concentrations. The SPCE emission intensities after addition of labeled antibody are shown in Fig. 10. The signal rapidly increases during the first few minutes and grows slowly during the next 10 min. As shown in Fig. 10A, the background signal (0 μg/L), representing nonspecific binding, is definitely much lower than for the lowest Myo concentration used, 50 μg/L, which is below the clinical cutoff Myo concentration of 90 μg/L for healthy patients.

We also examined the influence of human serum and 17% hemoglobin solution on the sensitivity of our Myo assay in a 1.0-mm–thick sample (not shown). Because signal attenuation was only 2- and 3-fold in serum and hemoglobin solution, respectively, a subclinical Myo concentration at 50 μg/L was readily detectable in those optically dense media.

Analytical assay characteristics, such as precision, accuracy, specificity, LODs, limits of quantification, and linearity, may depend on numerous factors, including analyte–antibody characteristics (such as Myo concentration and antibody affinity), assay conditions (such as temperature and incubation time), and such characteristics as slide substrate (metal layer coverage and protective SiO_2 layer) property variations. We demonstrated the applicability of SPCE technology to a real immunoassay within a clinically important cardiac marker concentration range. We did not seek to optimize the assay, which will be the topic of further investigation; however, the accuracy of the SPCE assay related solely to signal detection can be estimated. The variation in measured Myo concentration because of the signal detection accu-

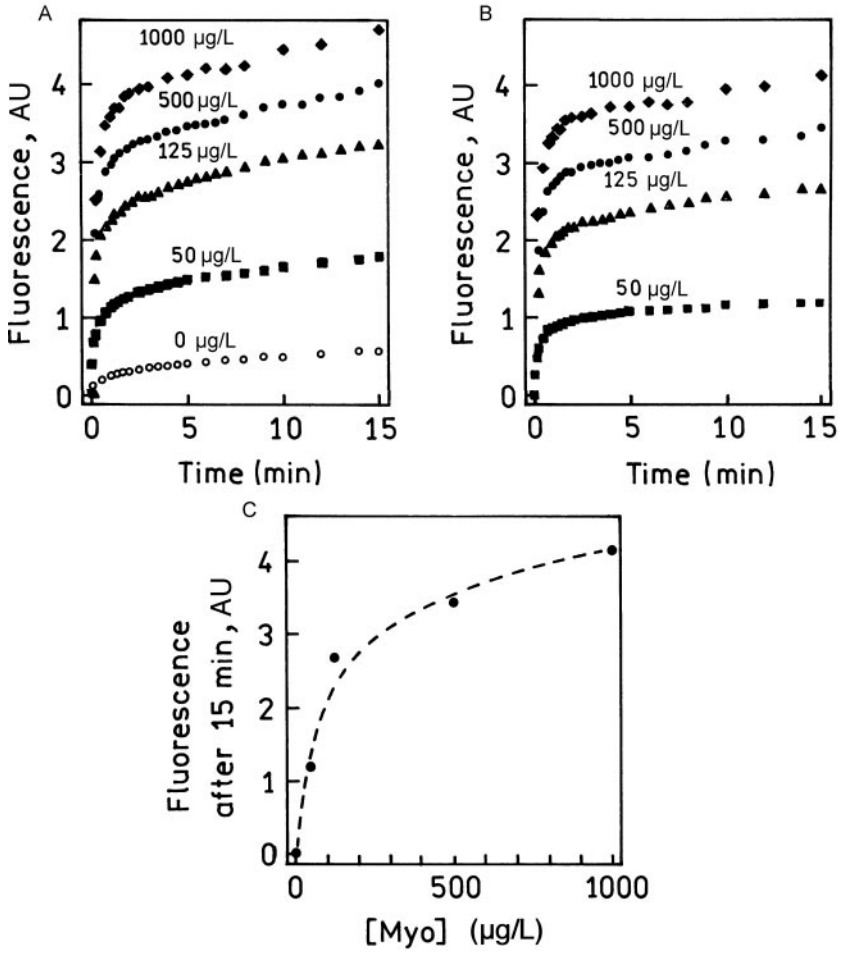

Fig. 10. Kinetics of Myo assay.

(*A* and *B*), kinetics of binding of the Rhodamine Red-X–labeled anti-Myo antibodies to myoglobin (0–1000 μg/L) captured on the 50-nm silver mirror surface observed in KR/SPCE configuration: (*A*), uncorrected data; (*B*), data after subtraction of background. (*C*), dependence of SPCE signal (after 15 min) on the Myo concentration. *Dashed line* represents the log trend (linear at log Myo concentration scale). *AU*, arbitrary units. Adapted from Matveeva et al. *(54)*.

racy, which was 2% or better, was <5% at Myo concentrations of 50 and 125 μg/L and <10% at Myo concentrations of 500 and 1000 μg/L, based on the semilog trend line covering the full range of Myo concentration studied (Fig. 10C).

Conclusions

SPCE immunoassays using the novel plasmonic approach described here may provide the following advantages over other fluorescence-based methods:

- Directional, rather than isotropic, emission is easy to detect with high collection efficiency.
- Background suppression is possible because only fluorophores within 200 nm of the metal couple to surface plasmons. The bulk fluorescence is rejected (reflected from the mirror).
- Simultaneous monitoring of different markers is possible. Because of the intrinsic dispersive properties of SPCE, the angle of directional emission depends on the emission wavelength (color) of the fluorophore. It is easy to collect angle-separated SPCEs.
- SPCE-based immunoassays can be performed in optically dense media, such as whole blood.

The proposed approach requires no washing steps and simplifies complex, heterogeneous assays. The SPCE measurements do not involve any sophisticated laser light sources and can be done with arc lamps or light emission diodes (LEDs). SPCE is also efficient because light excitation is not needed for the coupling of excitation to the surface plasmons; electroluminescence can lead to an efficient SPCE *(55)*.

This work was supported by the National Center for Research Resources (Grant RR-08119) and the National Institute of Biomedical Imaging and Bioengineering (Grant EB-00682).

References

1. Storrow AB, Gibler WB. The role of cardiac markers in the emergency department. Clin Chim Acta 1999;284:187–96.
2. Panteghini M, Apple FS, Christenson RH, Dati F, Mair J, Wu AH. Use of biochemical markers in acute coronary syndromes. IFCC Scientific Division, Committee on Standardization of Markers of Cardiac Damage. International Federation of Clinical Chemistry. Clin Chem Lab Med 1999;37:687–93.
3. Woo J, Lacbawan FL, Sunheimer R, LeFever D, McCabe JB. Is myoglobin useful in the diagnosis of acute myocardial infarction in the emergency department setting? Am J Clin Pathol 1995;103: 725–9.
4. Tucker JF, Collins RA, Anderson AJ, Hess M, Farley IM, Hagemann DA, et al. Value of serial myoglobin levels in the early diagnosis of patients admitted for acute myocardial infarction. Ann Emerg Med 1994;24:704–8.
5. Montague C, Kircher T. Myoglobin in the early evaluation of acute chest pain. Am J Clin Pathol 1995;104:472–6.
6. Kilpatrick WS, Wosornu D, McGuinness JB, Glen AC. Early diagnosis of acute myocardial infarction: CK-MB and myoglobin compared. Ann Clin Biochem 1993;30:435–8.
7. Ellenius J, Groth T, Lindahl B, Wallentin L. Early assessment of patients with suspected acute myocardial infarction by biochemical monitoring and neural network analysis. Clin Chem 1997;43: 1919–25.
8. Karras DJ, Kane DL. Serum markers in the emergency department diagnosis of acute myocardial infarction. Emerg Med Clin North Am 2001;19:321–37.
9. Newby LK, Storrow AB, Gibler WB, Garvey JL, Tucker JF, Kaplan AL, et al. Bedside multimarker testing for risk stratification in chest pain units: the chest pain evaluation by creatine kinase-MB, myoglobin, and troponin I (CHECKMATE) study. Circulation 2001; 103:1832–7.
10. McCord J, Nowak RM, Hudson MP, McCullough PA, Tomlanovich MC, Jacobsen G, et al. The prognostic significance of serial myoglobin, troponin I, and creatine kinase-MB measurements in patients evaluated in the emergency department for acute coronary syndrome. Ann Emerg Med 2003;42:343–50.
11. Panteghini M. Recent approaches in standardization of cardiac markers. Clin Chim Acta 2001;311:19–25.
12. Gordon Malan P. Immunological biosensors. In: Wild D, ed. The immunoassay handbook. New York: Nature Publishing Group, 2001:229–39.
13. Gosling JP. A decade of development in immunoassay methodology. Clin Chem 1990;36:1408–27.
14. van Dyke K, van Dyke R, eds. Luminescence immunoassay and molecular applications. New York: CRC Press, 1990:352pp.
15. Hemmila IA. Applications of fluorescence in immunoassays. New York: John Wiley & Sons, 1991:358pp.
16. Vo-Dinh T, Sepaniak MJ, Griffin GD, Alarie JP. Immunosensors: principles and applications. Immunomethods 1993;3:85–92.
17. Dandliker WB, de Saussure VA. Fluorescence polarization in immunochemistry. Immunochemistry 1970;7:799–828.
18. Fiore M, Mitchell J, Doan T, Nelson R, Winter G, Grandone C, et al. The Abbott IMx™ automated benchtop immunochemistry analyzer system. Clin Chem 1988;34:1726–32.
19. Klein C, Batz H-G, Draeger B, Guder H-J, Herrmann R, Josel H-P, et al. Fluorescence polarization immunoassay. In: Wolfbeis OS, ed. Fluorescence spectroscopy: new methods and applications. Berlin: Springer-Verlag, 1993:245–58.
20. Nasir MS, Jolley ME. Fluorescence polarization: an analytical tool for immunoassay and drug discovery. Comb Chem High Throughput Screen 1999;2:177–90.
21. Gomez-Hens A, Aguilar-Caballos MP. Stopped-flow fluorescence polarization immunoassay. Comb Chem High Throughput Screen 2003;6:177–82.
22. Morrison LE. Time-resolved detection of energy transfer: theory and application to immunoassays. Anal Biochem 1988;174:101–20.
23. Ullman EF, Schwarzberg M, Rubenstein KE. Fluorescent excitation transfer immunoassay: a general method for determination of antigens. J Biol Chem 1976;251:4172–8.
24. Qin QP, Peltola O, Pettersson K. Time-resolved fluorescence resonance energy transfer assay for point-of-care testing of urinary albumin. Clin Chem 2003;49:1105–13.
25. Soini E. Pulsed light, time-resolved fluorometric immunoassay. In: Bizollon CA, ed. Monoclonal antibodies and new trends in immunoassays. New York: Elsevier Science Publishers, 1984:197–208.
26. Diamandis EP. Immunoassays with time-resolved fluorescence spectroscopy: principles and applications. Clin Biochem 1988; 21:139–50.
27. Lövgren T, Pettersson K. Time-resolved fluoroimmunoassay, advantages and limitations. In: van Dyke K, van Dyke R, eds.

Luminescence immunoassay and molecular applications. New York: CRC Press, 1990:234–50.
28. Mathis G. Rare earth cryptates and homogeneous fluoroimmunoassays with human sera. Clin Chem 1993;39:1953–9.
29. Baker GA, Pandey S, Bright FV. Extending the reach of immunoassays to optically dense specimens by using two-photon excited fluorescence polarization. Anal Chem 2000;72:5748–52.
30. Waris ME, Meltola NJ, Soini JT, Soini E, Peltola OJ, Hanninen PE. Two-photon excitation fluorometric measurement of homogeneous microparticle immunoassay for C-reactive protein. Anal Biochem 2002;309:67–74.
31. Hanninen P, Waris M, Kettunen M, Soini E. Reaction kinetics of a two-photon excitation microparticle based immunoassay—from modeling to practice. Biophys Chem 2003;105:23–8.
32. Ekins RP, Chu FW. Multianalyte microspot immunoassay—microanalytical "compact disk" of the future. Clin Chem 1991;37:1955–67.
33. Bernard A, Michel B, Delamarche E. Micromosaic immunoassays. Anal Chem 2001;73:8–12.
34. Schobel U, Coille I, Brecht A, Steinwand M, Gauglitz G. Miniaturization of a homogeneous fluorescence immunoassay based on energy transfer using nanotiter plates as high-density sample carriers. Anal Chem 2001;73:5172–9.
35. Eggeling C, Brand L, Ullmann D, Jager S. Highly sensitive fluorescence detection technology currently available for HTS. Drug Discov Today 2003;8:632–41.
36. Lakowicz JR. Radiative decay engineering 3. Surface plasmon-coupled directional emission. Anal Biochem 2004;324:153–69.
37. Gryczynski I, Malicka J, Gryczynski Z, Lakowicz JR. Radiative decay engineering 4. Experimental studies of surface plasmon-coupled directional emission. Anal Biochem 2004;324:170–82.
38. Raether H. Surface plasma oscillations and their applications. In: Hass G, Francombe MH, Hoffman RW, eds. Physics of thin films, advances in research and development, Vol. 9. New York: Academic Press, 1977:145–261.
39. Pockrand I. Surface plasma oscillations at silver surfaces with thin transparent and absorbing coatings. Surf Sci 1978;72:577–88.
40. Lakowicz JR. Radiative decay engineering 5: metal-enhanced fluorescence and plasmon emission. Anal Biochem 2005;337:171–94.
41. Liebermann T, Knoll W. Surface-plasmon field-enhanced fluorescence spectroscopy. Colloids Surfaces A 2000;171:115–30.
42. Malicka J, Gryczynski I, Gryczynski Z, Lakowicz JR. DNA hybridization using surface plasmon-coupled emission. Anal Chem 2003;75:6629–33.
43. Gryczynski I, Malicka J, Lukomska J, Gryczynski Z, Lakowicz JR. Surface plasmon-coupled polarized emission of *N*-acetyl-L-tryptophanamide. Photochem Photobiol 2004;80:482–5.
44. Gryczynski I, Malicka J, Jiang W, Fischer H, Chan WCW, Gryczynski Z, et al. Surface plasmon-coupled emission of quantum dots. J Phys Chem B 2005;109:1088–93.
45. Yu F, Persson B, Lofas S, Knoll W. Surface plasmon fluorescence immunoassay of free prostate-specific antigen in human plasma at the femtomolar level. Anal Chem 2004;76:6765–70.
46. Ekgasit S, Stengel G, Knoll W. Concentration of dye-labeled nucleotides incorporated into DNA determined by surface plasmon resonance-surface plasmon fluorescence spectroscopy. Anal Chem 2004;76:4747–55.
47. Yu F, Persson B, Lofas S, Knoll W. Attomolar sensitivity in bioassays based on surface plasmon fluorescence spectroscopy. J Am Chem Soc 2004;126:8902–3.
48. Matveeva E, Gryczynski Z, Gryczynski I, Lakowicz JR. Immunoassays based on directional surface plasmon-coupled emission. J Immunol Methods 2004;286:133–40.
49. Gryczynski I, Malicka J, Nowaczyk K, Gryczynski Z, Lakowicz JR. Effects of sample thickness on the optical properties of surface plasmon-coupled emission. J Phys Chem B 2004;108:12073–83.
50. Matveeva E, Malicka J, Gryczynski I, Gryczynski Z, Lakowicz JR. Multi-wavelength immunoassay using surface plasmon-coupled emission. Biochem Biophys Res Commun 2004;313:721–6.
51. Nelson BP, Frutos AG, Brockman JM, Corn RM. Near-infrared surface plasmon resonance measurements of ultrathin films. 1. Angle shift and SPR imaging experiments. Anal Chem 1999;71:3928–34.
52. TFCalc [Computer Software]. Portland, OR: Software Spectra, Inc.
53. Matveeva E, Gryczynski Z, Malicka J, Lukomska J, Makowiec S, Berndt KW, et al. Directional surface plasmon-coupled emission—application for an immunoassay in whole blood. Anal Biochem, in press.
54. Matveeva E, Gryczynski Z, Gryczynski I, Malicka J, Lakowicz JR. Myoglobin immunoassay utilizing directional surface plasmon-coupled emission. Anal Chem 2004;76:6287–92.
55. Zhang J, Gryczynski Z, Lakowicz JR. First observation of surface plasmon-coupled electrochemiluminescence. Chem Phys Lett 2004;393:483–7.